

# Modeling the statistical distributions of cosmogenic exposure dates from moraines

P. J. Applegate<sup>1,\*</sup>, N. M. Urban<sup>1</sup>, K. Keller<sup>1</sup>, and R. B. Alley<sup>1</sup>

[1]{Department of Geosciences, Pennsylvania State University, University Park, Pennsylvania, 16801, United States}

[\*]{now at: Department of Physical Geography and Quaternary Geology, Stockholm University, SE-106 91 Stockholm, Sweden}

Correspondence to: P. J. Applegate (papplega@geosc.psu.edu)

## Abstract

Cosmogenic exposure dating provides a method for estimating the ages of glacial moraines deposited in the last ~100,000 years. Cosmic rays break atoms in surface rocks at predictable rates. Thus, the ages of moraines are directly related to the concentrations of cosmic ray-produced nuclides in rocks on the moraine surfaces, under ideal circumstances. However, many geomorphic processes may interfere with cosmogenic exposure dating. Because of these processes, boulders sometimes arrive at the moraines with preexisting concentrations of cosmogenic nuclides, or else the boulders are partly shielded from cosmic rays following deposition. Many methods for estimating moraine ages from cosmogenic exposure dates exist in the literature, but we cannot assess the appropriateness of these methods without knowing the parent distribution from which the dates were drawn on each moraine. Here, we make two contributions. First, we describe numerical models of two geomorphic processes, moraine degradation and inheritance, and their effects on cosmogenic exposure dating. Second, we assess the robustness of various simple methods for estimating the ages of moraines from collections of cosmogenic exposure dates. Our models estimate the probability distributions of cosmogenic exposure dates that we would obtain from moraine boulders with specified geomorphic histories, using Monte Carlo methods. We expand on pioneering modeling efforts to address this problem by placing these models into a common framework. We also evaluate the sensitivity of the models to changes in their input

parameters. The sensitivity tests show that moraine degradation consistently produces left-skewed distributions of exposure dates; that is, the distributions have long tails toward the young end of the distribution. In contrast, inheritance produces right-skewed distributions that have long tails toward the old side of the distribution. Given representative distributions from these two models, we can determine which methods of estimating moraine ages are most successful in recovering the correct age for test cases where this value is known. The mean is a poor estimator of moraine age for data sets drawn from skewed parent distributions, and excluding outliers before calculating the mean does not improve this mismatch. The extreme estimators (youngest date and oldest date) perform well under specific circumstances, but fail in other cases. We suggest a simple estimator that uses the skewnesses of individual data sets to determine whether the youngest date, mean, or oldest date will provide the best estimate of moraine age. Although this method is perhaps the most globally robust of the estimators we tested, it sometimes fails spectacularly. The failure of simple methods to provide accurate estimates of moraine age points toward a need for more sophisticated statistical treatments. We present improved methods for estimating moraine ages in a companion paper.

## 1 Introduction

Cosmogenic exposure dating is an important technique for learning about glacier size changes during the last  $\sim 10^5$  yr of geologic time (Gosse and Phillips, 2001). Glaciers and ice sheets grow and shrink in response to climate change (Dyurgerov and Meier, 2000; Oerlemans, 2005; Jansen et al., 2007). Therefore, reconstructions of past glacier sizes over time yield information on past climates and rates of sea level rise. As glaciers advance and retreat, they mark their former margins with ridges of debris, called moraines (Gibbons et al., 1984). In cosmogenic exposure dating, field geomorphologists collect samples from boulders on the crests of moraines, and the concentrations of certain rare chemical species (cosmogenic nuclides) are measured in the samples. These cosmogenic nuclides are produced at predictable rates in surface materials by cosmic rays (Lal, 1991; Gosse and Phillips, 2001). Under ideal conditions, the ages of the moraines can be calculated directly from the nuclide concentrations (e.g., Gosse et al., 1995a).

Unfortunately, geomorphic processes bias cosmogenic exposure dates (see review in Ivy-Ochs et al., 2007). If the boulders contain some preexisting concentration of cosmogenic nuclides when they are deposited on the moraine, then the exposure dates will tend to

overestimate the moraine's age. Most other processes tend to reduce the apparent exposure times of the boulders. For example, cover by snow or sediment reduces the flux of cosmic rays through the upper surfaces of the boulders. The exposure dates from these shielded boulders will underestimate the true age of the moraine on which they rest. Similarly, erosion of boulders removes the most nuclide-rich part of the rocks (Lal, 1991); therefore, eroded boulders also yield exposure dates that underestimate the age of their host moraine.

The effects of these processes on the distributions of exposure dates from moraines are not known *a priori*, and this lack of knowledge complicates efforts to estimate the ages of moraines from cosmogenic exposure dates. This uncertainty is reflected in the variety of procedures for estimating the ages of moraines that are described in the literature. Many workers prefer to use some measure of the central tendency of a data set; such estimators include the arithmetic average, the mean weighted by the inverse variance, and the mode (e.g., Kaplan et al., 2005; Licciardi et al., 2004; Kelly et al., 2008). Other investigators prefer extreme estimators, including both the youngest and the oldest dates (e.g., Benson et al., 2005; Briner et al., 2005). For data sets with large ranges, the choice of estimator has a profound effect on the estimated ages of the moraines (for example, compare Chevalier et al., 2005, with Brown et al., 2005). The choice of estimator is typically informed by geomorphic observations. However, without knowledge of the underlying parent distribution from which the dates are drawn, we cannot evaluate the effectiveness of these different procedures.

We might evaluate the effects of geomorphic processes on cosmogenic exposure dating by performing a positive control experiment. In such an experiment, we would identify a moraine whose age was known independently, perhaps from bracketing radiocarbon dates (e.g., Kowalski et al., in preparation). We would then collect many samples from this moraine for cosmogenic exposure dating, and compare a histogram of the exposure dates to the independently known age of the moraine. The distribution of the exposure dates about the true age of the moraine would tell us the effects of geomorphology on the exposure dates from that moraine, other factors being equal.

Unfortunately, such a positive control experiment is impractical. To achieve robust results, we would need many samples from one moraine. The exact number of samples required is poorly defined, but it seems likely that 50 samples are insufficient (see Murphy, 1964, his Fig. 6). Because cosmogenic exposure dates are expensive, the necessary number of samples is probably not achievable. In addition, the geomorphic processes that affect exposure dating

are likely to be highly variable between field sites. Thus, we would need to repeat the experiment on a large sample of moraines, multiplying the cost many times. Moreover, there are few sites where the ages of moraines are known independently, and these sites are already included in the nuclide production rate calibration database (Balco et al., 2008). Last, there are potential confounding effects. The difference between the independently determined age of a moraine and any individual exposure date is influenced by errors in estimating both the age of the moraine and the local production rates of cosmogenic nuclides. These errors interfere with our ability to separate out the effects of geomorphology on exposure dating. Thus, a positive control experiment to isolate the effects of geomorphic processes on exposure dating is prohibitively expensive, probably cannot be done for a representative sample of moraines, and is subject to strong confounding effects from uncertainties in moraine age estimates and nuclide production rates.

Monte Carlo-based numerical models offer a means of assessing the effects of geomorphic processes on cosmogenic exposure dating that avoids the disadvantages of positive control experiments. Although these models can never replace field observations, they provide a test bed for understanding existing exposure dates. Such models can generate thousands of synthetic exposure dates in a few minutes on desktop computers. Thus, these models do not have the large costs associated with collecting a representative number of samples from individual moraines. In these models, the user prescribes the age of the moraine and the nuclide production rate. Therefore, there are no confounding effects in the model experiments from errors in estimating these values.

In this paper, we present Monte Carlo models of two geomorphic processes that introduce biases into exposure dating. These processes are moraine degradation and inheritance, which we describe below. Our models are based on earlier work (e.g., Zreda et al., 1994; Hallet and Putkonen, 1994; Putkonen and Swanson, 2003; Benson et al., 2005; see also Muzikar, 2009). We expand on these groundbreaking studies in several ways. First, we provide explicit descriptions of the mathematical formulations of the models, pointing out the simplifying assumptions that are inherent in these formulations. We test the models' sensitivity to changes in their input parameters. Last, we provide code for these models that is written in MATLAB, an easily understood, high-level programming language.

In a companion paper (Applegate et al., in preparation; see also Applegate, 2009), we describe methods for making explicit comparisons between the output of our models and individual

data sets. This comparison can indicate which of the two processes we treat here is dominant on a particular moraine. More importantly, this inverse modeling procedure yields explicit estimates of moraine age, as well as other model parameters.

## **2 Methods**

### **2.1 Numerical models**

We describe models of two geomorphic processes that influence cosmogenic exposure dates from moraine boulders. These processes are moraine degradation and inheritance. In this section, we describe how our models treat these two processes, and we present preliminary results from these models.

These models are deliberately simplified. In theory, we could build a comprehensive model of moraine geomorphology that would incorporate all of the processes that influence exposure dates on moraines. However, we wish to invert these models against observations, to allow direct estimation of moraine ages from collections of cosmogenic exposure dates (Applegate et al., in preparation; see also Applegate, 2009). In a model inversion, the maximum number of model parameters that can be estimated from a data set is typically smaller than the number of observations. Our models have three to five parameters each, and most collections of cosmogenic exposure dates from moraines contain about five observations (Putkonen and Swanson, 2003). Therefore, our models are already at the complexity limit imposed by the sizes of most available data sets.

In any case, the usefulness of our models should be evaluated by confronting them with data (Box and Draper, 1987; Hilborn and Mangel, 1997). We describe this confrontation between our models and exposure dates from the literature in the companion paper (Applegate et al., in preparation; see also Applegate, 2009). We find that the models described in this paper are able to reproduce selected data sets from the literature. This finding suggests that we have identified the most important processes that influence exposure dating on moraines.

#### **2.1.1 The moraine degradation model**

In moraine degradation (Fig. 1), slope processes remove material from the crests of moraines and redeposit this material at the bases of the moraine slopes. The theoretical basis for understanding the redistribution of sediment on moraine slopes comes from observations

made on fault scarps, wave-cut bluffs, and other landforms composed of unconsolidated sediment. These landforms become less steeply inclined and more rounded over time, suggesting that hillslope evolution can be modeled as a diffusive process (Nash, 1986; Hanks, 2000; Pelletier et al., 2006; Pelletier, 2008). That is, material moves downhill at a rate that is proportional to the local gradient. This observation implies that a sharp-crested moraine will become shorter over its lifetime, as material moves from the moraine's crest to the toe of its slope (Anderson and Humphrey, 1989; Hallet and Putkonen, 1994; O'Neal, 2006; Putkonen et al., 2007; Pelletier, 2008). In this paper, the word *short* refers to the vertical dimension.

Moraine degradation imparts a bias to cosmogenic exposure dates because it exposes boulders at the moraine crest that have been buried in sediment for some part of the moraine's history (Fig. 1). Moraines typically contain large rocks distributed throughout a fine-grained matrix (Dreimanis, 1988; Benn and Evans, 1998). Because slope processes preferentially move fine-grained material, the boulders become concentrated on the crest of the moraine. Some of these boulders have been partly shielded from cosmic rays by the overlying sediment; they therefore contain smaller concentrations of cosmogenic nuclides than the boulders that have rested on the moraine crests since deposition of the moraine. The exhumed boulders yield cosmogenic exposure dates that underestimate the age of the moraine.

The model framework that we describe here builds on earlier studies. The use of slope evolution models to study moraines was first considered by Anderson and Humphrey (1989); Zreda et al. (1994) developed a model for the production of nuclides in boulders buried in an eroding surface. The first model of cosmogenic nuclide production on a diffusively evolving moraine was presented by Hallet and Putkonen (1994). This model was later developed further by Putkonen and Swanson (2003). Our model is closest to that of Putkonen and Swanson (2003).

To model the effects of slope processes on the height of moraines over time, we assume that moraines have an initial cross-section that is triangular, with an initial height  $h_0$  and an initial slope  $S_0$ , which is the (dimensionless) tangent of the slope in degrees. This profile evolves over time according to the one-dimensional diffusion equation,

$$\frac{\partial z}{\partial t} = k \frac{\partial^2 z}{\partial x^2}$$

(Hanks, 2000), where  $z(x, t)$  is the height of the moraine as a function of horizontal distance from the moraine crest  $x$  and time  $t$ ;  $k$  is the topographic diffusivity ( $\text{m}^2/\text{yr}$ ). This rule

assumes that  $k$  is constant over  $t$  and  $x$  (Pelletier et al., 2006; cf. Hallet and Putkonen, 1994; Roering et al., 2001). Solving this differential equation with our “sawtooth” initial moraine profile yields

$$z(x,t) = \frac{h_0}{2L} \left[ \left( \frac{2\sqrt{kt}}{\sqrt{\pi}} \right) z_1 + z_2 \right], \quad (1)$$

where

$$L = \frac{h_0}{S_0},$$

$$z_1 = \exp\left[\frac{-(L+x)^2}{4kt}\right] - 2\exp\left(\frac{-x^2}{4kt}\right) + \exp\left[\frac{-(L-x)^2}{4kt}\right], \text{ and}$$

$$z_2 = (L+x)\operatorname{erf}\left(\frac{L+x}{2\sqrt{kt}}\right) - 2x\operatorname{erf}\left(\frac{x}{2\sqrt{kt}}\right) + (L-x)\operatorname{erf}\left(\frac{L-x}{2\sqrt{kt}}\right)$$

(cf. Pelletier, 2008, his eqn. 2.45). Equation 1 agrees well with a Crank-Nicolson solution to equation 4 of Hallet and Putkonen (1994) if their  $\beta = 0$ ; compare equation 4 of Hallet and Putkonen (1994) to equations 9.56 and 9.67 of Fletcher (1991). This analytical solution can be evaluated very quickly.

Setting  $x = 0$  in equation 1 yields an expression for the height of the moraine’s crest as a function of time,

$$h(t) = \frac{h_0}{L} \left\{ \left( \frac{2\sqrt{kt}}{\sqrt{\pi}} \right) \left[ \exp\left(\frac{-L^2}{4kt}\right) - 1 \right] + L\operatorname{erf}\left(\frac{L}{2\sqrt{kt}}\right) \right\}. \quad (2)$$

Figure 2 shows solutions to equations 1 and 2 for selected parameter values. The left panel (Fig. 2a) shows the moraine half-profile for elapsed time values of 5 ka, 10 ka, and 20 ka. The moraine starts with a triangular profile, but becomes more rounded and shorter over time. The right panel (Fig. 2b) shows the height of the moraine as a function of time. The rate of crest lowering is rapid at first, then slows. In both panels, the initial moraine height is 50 m, the initial moraine slope is  $34^\circ$  (Putkonen and Swanson, 2003), and the topographic diffusivity is  $10^{-2} \text{ m}^2/\text{yr}$  (Hanks, 2000; Putkonen et al., 2007). These values seem reasonable for the large, last-glacial moraines of the western United States.

Given equation 2, we can calculate the nuclide concentration in a boulder buried to some specified depth  $d_0$  below the moraine’s surface at the time of deposition. For purposes of calculating nuclide production rates, the depth of a boulder  $d(t)$  is given by

$$d(t) = h(t) - (h_0 - d_0) \quad \text{for } h(t) \geq h_0 - d_0, \text{ and}$$

$$d(t) = 0 \quad \text{for } h(t) < h_0 - d_0.$$

Note that  $d_0$  and  $d$  here refer to the depth of the top of the boulder, which is the point that will be sampled for cosmogenic nuclide measurements.

Values of  $d_0$  that exceed  $h_0 - h_f$  are not meaningful, because these boulders will still be buried in the moraine at the time of sampling. By  $h_f$ , we mean the final height of the moraine, achieved when  $t$  reaches the moraine's age. In addition, field geomorphologists typically do not sample boulders that stand less than some minimum height  $h_b$  above the moraine crest ( $\sim 1$  m; e.g., Gosse et al., 1995b). Thus, all the boulders that are sampled have values of  $d_0$  that satisfy the criterion

$$0 \leq d_0 \leq \max(d_0);$$

$$\max(d_0) = h_0 - h_f - h_b.$$

The production rate of most cosmogenic nuclides declines exponentially as a function of depth below material surfaces (Lal, 1991; see Zreda et al., 1994, for an important exception). That is,

$$P(d) = P_0 \exp\left(\frac{-d}{\Lambda}\right), \quad (3)$$

where  $P_0$  is the production rate of the nuclide at the surface (atoms/g rock/yr), and  $\Lambda$  is the attenuation length of cosmic rays in the material ( $\sim 160$  g/cm<sup>2</sup>, divided by the material's density). We use the Lal/Stone production rates from the CRONUS online calculator (Balco et al., 2008) to estimate  $P_0$ .

Equation 3 is a good approximation only at shallow depths, where nucleon production dominates; at greater values of  $d(t)$ , muon production becomes important (Gosse and Phillips, 2001). To account for muon production, we use the parameterization of Granger and Muzikar (2001, their eqns. 1-3). This scheme represents production at a given depth as the sum of four exponential terms, each with its own  $P_0$  and  $\Lambda$ . That is,

$$P(d) = \sum_{i=1}^4 P_i \exp\left(\frac{-d}{\Lambda_i}\right). \quad (4)$$

We scale these terms relative to their values at sea level and high latitude, again using the CRONUS online calculator (Balco et al., 2008). This expression is a parameterization; Heisinger et al. (2002a, 2002b) present alternative expressions that resolve the underlying physics. We use the relationship presented in equation 4 because it can be evaluated very

quickly as a vector calculation in MATLAB. The speed of evaluation is important because this calculation must be performed approximately  $10^7$  times for each forward run of this model (see below).

Figure 3a shows the production rate of the cosmogenic nuclide beryllium-10 as a function of depth. Nucleon production dwarfs muon production at the surface, but muon production becomes increasingly important at greater depths (Fig. 3b).

Given equations 2 and 4, we can calculate the final concentration of cosmogenic nuclides in a moraine boulder. This calculation depends only on the moraine's initial geometry ( $h_0, S_0$ ), its age, its topographic diffusivity  $k$ , and the boulder's initial depth  $d_0$ . However, the production rate in a given boulder is a piecewise function of time, because the production rate stops changing when the boulder breaks the surface of the moraine (that is, when  $d$  becomes 0; Fig. 4b). Therefore, we break the lifetime of the moraine into  $n$  time steps, each having a duration  $\Delta t$ . We then evaluate the change in concentration during each of these time steps. The final concentration  $C_f$  in any single boulder is the sum of the changes in concentration during the individual time steps, or

$$C_f = \sum_{i=1}^n \{P(t)\Delta t - C_{i-1}[1 - \exp(-\lambda\Delta t)]\} \quad (5)$$

(Lal, 1991, his eqn. 6; cf. eqn. 6, below). The second term in brackets represents the progressive decay of unstable cosmogenic nuclides;  $\lambda$  is the decay constant of the appropriate nuclide ( $\text{yr}^{-1}$ ; Gosse and Phillips, 2001; Balco et al., 2008). The difference between this approximation and an exact solution can be made arbitrarily small by reducing  $\Delta t$ . For the model runs shown in this paper, we used values of  $\Delta t$  ranging from 25 yr to 100 yr. Note that the initial concentration  $C_0$  is taken to be zero here; we treat inheritance in the next section.

Figure 4a shows the depths of four boulders within the moraine as a function of time, assuming the same model parameters as in Figure 2. At the beginning of the simulation, one boulder is at the surface ( $d_0 = 0$  m), another boulder is buried to a depth of 9 m ( $d_0 = 9$  m), and the other two boulders are evenly spaced between these depths. As the moraine becomes shorter over time, the boulders approach the surface and are eventually exposed at the surface. Compare this figure to Figure 2b.

Figure 4b shows the concentrations of beryllium-10 as a function of time in each of the boulders whose depth trajectories are shown in Figure 4a. Again, the model parameters used to generate this figure are the same as those in Figure 2. The concentrations in the boulders

increase slowly while the boulders are still buried in the moraine; after they reach the surface, the concentration increases roughly in proportion to surface residence time. Although the curves that describe nuclide concentration in the boulders as a function of time appear to be linear after the boulders reach the surface, they are slightly sublinear because of nuclear decay (eqn. 5). Note that the bulk of the final nuclide concentration in each boulder is acquired only after the boulder reaches the surface, even for the boulder that is buried most deeply in the moraine at the beginning of the simulation. This figure assumes that the beryllium-10 concentrations in all the boulders are zero when the simulation begins.

Although we do not emphasize boulder erosion in this paper, the model treats erosion by the progressive removal of thin shells of material from boulder surfaces after they are exhumed from the till. In contrast to Hallet and Putkonen (1994), we do not allow boulders to shrink below the observed boulder height  $h_b$  (see Zreda et al., 1994). Instead, we determine the amount of time that each boulder will be exposed to surface weathering from equation 2, then specify initial sizes for the boulders that will result in the boulders having the observed height.

This model assumes that exhumed boulders do not topple or rotate as the crest of the moraine deflates. It also neglects the effects of cryoturbation (Lal and Chen, 2005). Toppling or rotation of boulders on a degrading moraine would produce a larger range of exposure dates than degradation alone, because these processes effectively reduce the measured nuclide concentrations in sampled boulders (Ivy-Ochs et al., 2007; Schaefer et al., 2008). Conversely, cryoturbation might bring boulders to the moraine surface sooner than would be predicted by diffusive removal of the moraine crest, thereby reducing the range of exposure dates from the moraine. In this paper, we assume that these processes are not dominant.

Some moraines have geomorphic characteristics that are inconsistent with the assumptions used in constructing the moraine degradation model. For example, it would be inappropriate to apply our model of moraine degradation to the large Pinedale terminal moraines near Pinedale, Wyoming (Richmond, 1973; Gosse et al., 1995a), particularly in the Halls Lake (Mud Lake) drainage. These moraines have broad, flat crests, where the local slope is close to zero. Consequently, the downhill flux of material at the crests of these moraines should be small. We expect that these moraines have lost little material from their crests over time. Moreover, limited exposures in roadcuts at Fremont Lake show that there are few or no boulders in the subsurface till (E. Evenson, personal communication). This observation

invalidates the assumption that the boulders are uniformly distributed throughout the outermost Pinedale-age moraine at Fremont Lake.

### 2.1.2 The inheritance model

Boulders that are deposited on a moraine with nonzero concentrations of cosmogenic nuclides are said to have inheritance. The inherited nuclides were produced in each boulder during one or several periods of “pre-exposure” (Ivy-Ochs et al., 2007). That is, the boulders were incompletely shielded from cosmic rays before being deposited on the moraine. These boulders contain larger concentrations of cosmogenic nuclides than boulders that were completely shielded from cosmic rays at all times before being incorporated into the moraine. Exposure dates from boulders with inherited nuclides tend to overestimate the age of the moraine.

There are at least two potential sources of pre-exposed boulders in glaciated landscapes (Ivy-Ochs et al., 2007). First, boulders may topple onto the glacier surface from cirque headwalls or adjacent, oversteepened valley walls (Seong et al., 2009). These boulders then ride the glacier’s surface to the terminus, where they fall onto the moraine. Second, glaciers may re-entrain boulders deposited in the valley bottom during an earlier advance, or pluck boulders from bedrock outcrops at the glacier bed. These boulders are then transported subglacially to the glacier terminus, where they may be emplaced at the moraine surface by thrusting (e.g., Kruger, 1996) or other ice-marginal processes.

The mathematical descriptions of these two situations are nearly identical. In both cases, the concentration measured in each boulder is the sum of the inherited component acquired during pre-exposure, and the post-depositional component that reflects the exposure history of the boulder after moraine construction.

The model that we describe here is based on an earlier model presented by Benson et al. (2005), which treated inheritance in boulders derived from cirque headwalls. Our model uses a mathematical formulation that is similar to the one used by Benson et al. (2005), but treats a larger set of geomorphic situations. In addition, our model of inheritance is similar to the model of nuclide concentrations in sediment over time used in cosmogenic burial dating (Granger et al., 2001; Granger and Muzikar, 2001). Following this pioneering work, we assume that the sampled clasts had two distinct periods of residence in the landscape, and that

the rate of change of nuclide concentrations in the clasts was different during these two periods.

For simplicity, we begin by describing the model treatment of inheritance in reworked boulders (Fig. 5). We then point out a slight change in the model formulation that allows it to treat inheritance in boulders derived from cirque headwalls and valley walls.

For reworked boulders, the inherited concentration in each boulder depends on the time between deposition of the boulder by the retreating ice and entrainment of the boulder by the readvancing glacier  $t_{pre}$ , and on how deeply the boulder was buried during this time  $d_{pre}$ . Both these parameters are unknown for any individual boulder, but it is reasonable to say that they must range from zero to some maximum.

$$0 \leq t_{pre} \leq \max(t_{pre}), \text{ and}$$

$$0 \leq d_{pre} \leq \max(d_{pre}).$$

The maximum time  $\max(t_{pre})$  represents the time between the beginning of the penultimate glacial retreat and the time of moraine deposition; the maximum depth  $\max(d_{pre})$  is the maximum thickness of material eroded by the glacier during its readvance.

Note that  $d_{pre}$  refers to the depth of the point on each boulder that is eventually sampled, not the top of the boulder, during the predepositional exposure time. Field geomorphologists typically sample the upper surfaces of boulders, because those surfaces receive the maximum flux of cosmic rays. However, glacial transport rotates boulders, and so the sample point is not necessarily the same as the apex of the boulder during the predepositional exposure time. Sampling of the sides of moraine boulders yields a range of nuclide concentrations (Schaefer et al., 2008), consistent with theoretical predictions of the distribution of nuclide production in solids (Masarik and Wieler, 2003; Lal and Chen, 2005).

For a boulder buried in a till sheet, equation 4 gives the production rate in the point that is eventually sampled. Given this production rate, the inherited concentration  $C_{pre}$  is

$$C_{pre} = \frac{P(d_{pre})}{\lambda} [1 - \exp(-\lambda t_{pre})]$$

(Lal, 1991, his eqn. 6), and the final concentration  $C_f$ , achieved after the boulder has rested on the moraine for a time  $t$ , is

$$C_f = C_{pre} \exp(-\lambda t) + \frac{P_0}{\lambda + \epsilon \Lambda^{-1}} [1 - \exp(-\lambda t)] \quad (6)$$

(Lal, 1991, his eqn. 6). Here,  $\varepsilon$  is the erosion rate of the boulders after they are delivered to the moraine (cm/yr; assumed negligible), and  $\Lambda$  is the attenuation length of the nucleonic component of cosmogenic nuclide production ( $\sim 160$  g/cm<sup>2</sup>, divided by the material's density; Lal, 1991; Gosse and Phillips, 2001).

Our model is readily adapted to treat inheritance in boulders derived from cirque headwalls and valley walls, as in Benson et al. (2005). From a nuclide production perspective, the angle of the overlying surface is the critical difference between a boulder buried in a till sheet and one that is still in a cirque headwall; for a till sheet, the overlying surface should be nearly horizontal, whereas cirque headwalls are quite steep. To model nuclide production as a function of depth below inclined surfaces, we use the parameterization of Dunne et al. (1999, their eqn. 18). This parameterization gives results within 3% of estimates from a more explicit model (Dunne et al., 1999), even for the steep slopes representative of cirque headwalls ( $\sim 30^\circ$ ; Benson et al., 2005).

The model implicitly accounts for the rotation of boulders during glacial transport. Because glacial transport mixes sediment and boulders, most previously exposed boulders will arrive on the moraine in a different orientation than they had during their predepositional exposure times. Thus, for a boulder shaped like a cube, there is a 1-in-6 chance that the face that is eventually sampled is the one with the largest concentration of inherited cosmogenic nuclides (Benson et al., 2005). Because our model is formulated in terms of the depth of the sampled point on each boulder below the predepositional exposure surface, the inherited nuclide concentrations are insensitive to the boulders' orientations during the predepositional exposure time. This statement will be true as long as the density contrast between the boulders and the surrounding material is small. If there is a large difference in density between the boulders and the surrounding material during the predepositional exposure period, the production rate in the sampled points will differ, depending on the orientations of the boulders.

This inheritance model relies on many assumptions. First, we assume that there are no nuclides inherited from any periods of residence in the landscape preceding the last glacial cycle. Because many cosmogenic nuclides have half-lives that are long compared to glacial cycles (Gosse and Phillips, 2001; Shackleton, 2000), this assumption requires that glaciers sweep out most of the easily eroded material from their valleys during each advance. Second, we assume that surface production rates were the same during the predepositional exposure

time as they are in the boulders' observed positions. Because some boulders are undoubtedly coming from higher elevations than the present-day moraine crests, this assumption tends to underestimate surface production rates during the predepositional exposure time. Future versions of this model will need to incorporate information on the elevation distribution of glaciated basins (e.g., Bierman et al., 2005). For boulders that travel to the moraine atop glacial ice, some cosmogenic nuclide atoms are produced during the transport time (Seong et al., 2009), and our model neglects this production. Moreover, glaciers do erode boulders during subglacial transport, and this model does not include that process. We tolerate these problems for the sake of developing this preliminary model.

## 2.2 Monte Carlo simulation

To determine a statistical distribution of apparent exposure dates from our models, we use Monte Carlo methods (Hilborn and Mangel, 1997; Bevington and Robinson, 2003). In Monte Carlo simulation, the values of highly variable model parameters are chosen randomly from predefined probability distributions. The model is then run for these parameter values, and the output is saved. This process is repeated many times; depending on the speed of the model and the desired precision, Monte Carlo model evaluations may include thousands to millions of individual model runs. The model output is then plotted as a histogram, which is a graphical representation of the probability distribution.

In our models, there are several free parameters that will be different for each boulder on a moraine. We have no way of determining, for example, how deeply buried any individual boulder was at the time of moraine deposition. The moraine degradation model has only one highly variable parameter, the initial depth  $d_0$ ; the inheritance model has two highly variable parameters, the predepositional exposure time  $t_{\text{pre}}$  and the depth during the predepositional exposure time  $d_{\text{pre}}$ .

Because all these free parameters range from zero to some maximum, we choose random values for these parameters from continuous uniform distributions. In a continuous uniform distribution, all real numbers that lie between the minimum and maximum ends of the distribution are equally probable (Hilborn and Mangel, 1997; Bevington and Robinson, 2003). For our models, the minimum ends of these distributions are always 0; the maximum ends are specified by  $\max(d_0)$ ,  $\max(t_{\text{pre}})$ , and  $\max(d_{\text{pre}})$ .

For each draw of these randomly chosen parameter values, we calculate the final concentration  $C_f$  (eqns. 5 and 6, above) and the apparent exposure time  $t_{app}$ , according to

$$t_{app} = \frac{-1}{\lambda} \ln \left( 1 - \frac{C_f \lambda}{P_0} \right) \quad (7)$$

(Lal, 1991, his eqn. 6). This expression reflects the “naïve” estimate (Wolkowinsky and Granger, 2004) of moraine age from a single boulder sample, neglecting boulder erosion and all other geomorphic processes.

Note that we differentiate between moraine-level parameters and boulder-level parameters. Moraine-level parameters in the degradation model include the moraine age, topographic diffusivity, initial height, and initial slope; in the inheritance model, the moraine-level parameters are the moraine age, the maximum predepositional exposure time, and the maximum predepositional burial depth. The boulder-level parameters are the initial depth of boulders below the moraine surface in the degradation model, and the predepositional exposure time and burial depth in the inheritance model. In estimating the probability distribution of cosmogenic exposure dates from a single moraine, we vary the boulder-level parameters, but the moraine-level parameters remain constant.

### 2.3 Plotting non-normal distributions

Many common methods of plotting collections of exposure dates from moraines implicitly assume that the dates are drawn from a normal distribution. This assumption is unjustified for the distributions produced by our models, which are clearly not normal. Therefore, we represent the statistical distributions of exposure dates using histograms, cumulative density functions, and box plots (Chambers et al., 1983; Croarkin and Tobias, 2006). These plotting methods are robust, even for statistical distributions that vary considerably from the normal distribution.

Histograms are probably the most familiar method of representing distributed data, but the choice of bin size exerts a strong control on the shape of the histogram. In a histogram, the synthetic observations are sorted into bins. The heights of the bars on the histogram are proportional to the number of observations in each bin.

Unlike histograms, plots of cumulative density functions do not require arbitrary choices about how to group the data. On a plot of a cumulative density function, the  $y$ -axis represents the probability that any individual observation is equal to or less than a particular value on the

$x$ -axis (Press et al., 1992, their ch. 14; Hilborn and Mangel, 1997; Croarkin and Tobias, 2006). The  $x$ -axis therefore ranges from the minimum to the maximum of the observations; the  $y$ -axis ranges from 0 to 1.0.

Box plots provide a compact way of representing distributed data; placing several box plots next to one another allows quick comparison of distributions. In a box plot, the position and width of the box indicates where the middle 50% of the observations lie. That is, the box represents the interquartile range of the data (Chambers et al., 1983; Croarkin and Tobias, 2006). The line in the box is the median, or the value that separates the lower half of the observations from the upper half. In this paper, the ends of the whiskers indicate the positions of the largest and smallest observations. Often, box plots indicate outliers as dots or small crosses outside the whiskers (Chambers et al., 1983), but we do not follow this practice.

### **3 Results**

#### **3.1 Model output for representative parameter values**

The output from the moraine degradation model is shown in Figure 6. All these figures assume the same parameter values used in Figures 2 and 4; as before, the initial height of the moraine is 50 m, the initial slope of the moraine is  $34^\circ$  (Putkonen and Swanson, 2003), the topographic diffusivity is  $10^{-2}$  m<sup>2</sup>/yr (Hanks et al., 2000; Putkonen et al., 2007), and the age of the moraine is 20 ka. In addition, we specify that the tops of all sampled boulders must be at least 1 m above the crest of the moraine at the time of sampling.

Figure 6a illustrates the relationship between the initial depth of a given boulder and the apparent exposure time yielded by that boulder. As expected, the more deeply buried samples yield younger apparent exposure times.

Figures 6b and 6c show the statistical distribution of the exposure dates produced by the degradation model for these parameter values. The distribution is strongly left-skewed; that is, more of the probability mass falls to the left of the distribution's peak than would be the case if the distribution were normal. The corresponding cumulative density function rises slowly, then more rapidly as it approaches the true age of the moraine (20 ka). The box portion of the box plot, which represents the position of the bulk of the data, falls on the right-hand side of the plot.

The output from the inheritance model is shown in Figures 7a-7c. These plots assume a moraine age of 20 ka, a maximum predepositional exposure time of 100 ka, a maximum depth during the predepositional exposure period of 2 m, an overburden density of 2.0 g/cm<sup>3</sup>, and a flat surface geometry during the predepositional exposure period. Again, the total number of synthetic observations in each of these plots is 10<sup>5</sup>.

Figure 7a shows contours of the apparent exposure time produced by the inheritance model as a function of the model's free parameters, predepositional exposure time and predepositional exposure depth. As expected, the samples that yield the greatest apparent exposure times are those that had the greatest length of time to acquire inherited nuclides and were near the surface during that time. That is, the samples that appear oldest have the longest predepositional exposure times and the smallest predepositional exposure depths.

Figures 7b and 7c show the statistical distributions of exposure dates expected from the inheritance model for these parameter values. The distribution is right-skewed; it contains a mode close to the true age of the moraine (20 ka), and a long, heavy tail to the old side, as shown in the histogram (Fig. 7b). These features of the distribution are reflected in the cumulative density function (Fig. 7c), which rises rapidly, then levels off. The box portion of the box plot falls near the left end of the plot.

### **3.2 Sensitivity of modeled distributions to input parameter values**

Some of the parameters used in our models are either highly uncertain, or else vary considerably between moraines. In this section, we show how the modeled distributions of exposure dates change as individual parameters vary. Figures 8 and 9 illustrate the sensitivity of the two models using box plots (Chambers et al., 1983).

In both models, the moraine age controls the position of the box plot along the time axis. In the inheritance model, the spread of the exposure dates is independent of moraine age; the distance between the ends of the whiskers is the same for all values of moraine age. In contrast, the moraine age does affect the spread of exposure dates yielded by the degradation model; that is, younger moraines show less spread than older moraines (Fig. 8; Putkonen and Swanson, 2003). The increase in spread among exposure dates with age for degrading moraines happens because older moraines have more time to lose material from their crests (Fig. 2), and this process exposes more boulders that have spent progressively less time exposed to the full surface flux of cosmic rays (Fig. 4).

In the degradation model, the spread of dates is most strongly controlled by the topographic diffusivity, although the initial slope and initial height of the moraine also have some influence on the scatter (Fig. 8). Small diffusivities cause the moraine's height to change only slightly over its lifetime, and so few new boulders are exhumed at the crest of the moraine. Very large diffusivities flatten the moraine in a few thousand years after its construction; the reduced spread in exposure dates produced by the model for a diffusivity of  $1 \text{ m}^2/\text{yr}$  happens because such a high diffusivity exposes most of the buried boulders within a few thousand years after the deposition of the moraine. Such large diffusivities cause the moraine to disappear almost totally over 20 ka, so they are inconsistent with the observed persistence in the landscape of topographically distinct moraines (see Hanks, 2000; Putkonen et al., 2007). The modeled distributions of exposure dates from tall moraines are wider than distributions from shorter moraines of the same age (Putkonen and Swanson, 2003), although the width of the distribution stops increasing as the initial height of the moraine is made greater than  $\sim 35$  m. The range of modeled exposure dates increases monotonically with the initial slope of the moraine.

In the inheritance model, the maximum predepositional exposure time controls the width of the distribution, and the maximum predepositional exposure depth controls where the bulk of the data falls between the extreme ends of the distribution (Fig. 9). A large value for the maximum predepositional exposure time causes a wide range of exposure dates; a small value produces a narrow range. Large values of the maximum predepositional exposure time concentrate most of the observations near the young end of the range, whereas smaller values place more of the observations into the tail of the distribution.

Increasing the surface slope has only a small effect on the distributions of exposure dates produced by the inheritance model (Fig. 9). There is little difference between the distributions of modeled exposure dates for boulders derived from flat surfaces and those for boulders derived from sloped surfaces with inclinations of  $30^\circ$  or less, because the depth dependence of nuclide production changes only slightly over this range of slopes (Dunne, 1999). A  $30^\circ$  slope is representative of cirque headwalls (Benson et al., 2005), a likely source for supraglacial boulders. The model sensitivity to surface slope is not extreme, even for larger slope values.

## 4 Discussion

There is no plausible combination of parameters that can cause the output from the moraine degradation model to resemble the output from the inheritance model (compare Fig. 6b with Fig. 7b, Fig. 6c with Fig. 7c, and Fig. 8 with Fig. 9), except in the special case where neither process is active. The statistical distributions of exposure dates produced by the moraine degradation model are always left-skewed (Fig. 6b); conversely, the distributions of exposure dates produced by the inheritance model are always right-skewed (Fig. 7b). That is, the cumulative density functions from the degradation model are always concave-up (Fig. 6c), and the cumulative density functions from the inheritance model are always concave-down (Fig. 7c). On the box plots, the box occurs near the right-hand end of the distribution in the degradation model (Fig. 8), and near the left-hand side of the plot for the inheritance model (Fig. 9).

We can now examine how successful different methods for estimating moraine ages will be, given the statistical distributions of exposure dates yielded by our models (Fig. 10). Common methods include the mean, the mean after discarding outliers, the oldest date, and the youngest date. In this case, we define outliers as those observations that are more than twice the standard deviation away from the mean of the exposure dates in a data set.

To this list of methods, we add the min/mean/max technique, which was suggested by our modeling results. If a data set has a skewness greater than 0.5, we infer that the dates are biased by inheritance, so we take the youngest date. If the skewness is less than -0.5, we assume moraine degradation, and take the oldest date. If the skewness is between -0.5 and 0.5, we take the mean.

Of these methods, min/mean/max appears to be the most widely applicable; however, none of these methods is universally successful in recovering the known ages of moraines for our modeled distributions (Fig. 10). The median of the min/max/mean age estimates always lies within a few thousand years of the true age for the parent distributions we examine here. This statement is not true of any other method that we have tested. However, the min/max/mean estimate of moraine age sometimes overestimates or underestimates moraine ages by tens of thousands of years.

The min/mean/max method fails because the skewness of a small data set ( $n < \sim 50$ ) is a poor guide to the form of the parent distribution (Fig. 11). For a moraine where geomorphic processes do not affect exposure dating, we would expect the exposure dates to be normally

distributed (Balco, in press), and to have a standard deviation equal to the measurement uncertainty of the dates. By definition, this parent distribution will have a skewness of zero. However, the skewness of a small number of exposure dates drawn randomly from this parent distribution has a poor chance of approximating the true skewness of the parent distribution. Most randomly selected data sets containing a small number of observations will give either a positive or negative skewness. Under the min/mean/max framework, we would wrongly conclude that we should take the oldest or the youngest date from these data sets, whereas the average is the maximum likelihood estimator of the moraine's age (Bevington and Robinson, 2003). This problem is most pronounced for the smallest data sets ( $n = 3$ ), for which the distribution of skewnesses is U-shaped.

These problems persist for data sets drawn from distributions generated by the inheritance model and the degradation model. For highly skewed parent distributions like those produced by the inheritance model, the interquartile range of sample skewnesses does not even overlap the skewness of the parent distribution until the number of observations in each data set is about 15. To our knowledge, there is no moraine with more than 15 independent, published cosmogenic exposure dates.

Taking the mean after discarding outliers fails to correctly estimate the ages of moraines for skewed parent distributions (Fig. 10) because the bias imparted by geomorphic processes is continuous, rather than binary. Discarding outliers before taking the mean implicitly assumes that bias is either present or absent in each exposure date. Our model results suggest, instead, that the majority of exposure dates from moraines that are affected by geomorphic processes have some degree of bias, even though small biases are more common than large ones (Figs. 6, 7; Benson et al., 2005). These small biases lead the mean away from the correct answer, if that answer lies at one end of the distribution.

The extreme estimators work well in very specific circumstances (Fig. 10), but we cannot reliably determine when to apply these estimators (Fig. 11). The extreme estimators involve choosing the youngest date or the oldest date from a data set. If we believe correctly that the parent distribution from which a set of exposure dates is drawn is skewed in one direction or the other, then the corresponding extreme estimator is the best choice for determining the moraine's age (Fig. 10). However, an incorrect guess about the form of the parent distribution will likely cause a large error in estimating the age of a moraine using an extreme

estimator. Because our skill in determining the form of parent distributions from small data sets is limited (Fig. 11), the extreme estimators should be used with caution.

The failure of simple methods to correctly estimate the ages of moraines in our test cases indicates that more sophisticated methods are necessary. Direct inversion of our models against data may allow more accurate estimation of moraine ages from collections of cosmogenic exposure dates. We present methods for this inversion in the companion paper (Applegate et al., in preparation; see also Applegate, 2009).

### **Acknowledgements**

This work was partly supported by the US National Science Foundation (grants 0531211, 0539578 and 0424589), and the Comer Science and Education Foundation. T. Lowell, D. Pollard, K. Peterson, A. Carleton, and B. Goehring provided helpful comments on drafts of this manuscript.

## References

- Anderson, R. S., and Humphrey, N. F.: Interaction of weathering and transport processes in the evolution of arid landscapes, in: Quantitative dynamic stratigraphy, Prentice-Hall, 349-361, 1989.
- Applegate, P. J.: Estimating the ages of glacial landforms from the statistical distributions of cosmogenic exposure dates, Ph. D. dissertation, Pennsylvania State University, United States, 2009.
- Applegate, P. J., Urban, N. M., Kelly, M. A., Lowell, T. V., Laabs, B. J. C., Keller, K., and Alley, R. B: Extracting moraine ages and geomorphic process information from the statistical distributions of cosmogenic exposure dates, *Geology*, in preparation.
- Balco, G., Stone, J. O., Lifton, N. A., and Dunai, T. J.: A complete and easily accessible means of calculating surface ages or erosion rates from  $^{10}\text{Be}$  and  $^{26}\text{Al}$  measurements, *Quat. Geochronol.*, 3, 174-195, 2008.
- Benn, D. I., and Evans, D. J. A.: *Glaciers and glaciation*, Hodder Arnold, 1998.
- Benson, L., Madole, R., Landis, G., and Gosse, J.: New data for late Pleistocene Pinedale alpine glaciation from southwestern Colorado, *Quaternary Sci. Rev.*, 24, 49-65, 2005.
- Bevington, P. R., and Robinson, D. K.: *Data reduction and error analysis for the physical sciences*, 2nd ed., McGraw-Hill, 336, 2003.
- Bierman, P. R., Reuter, J. M., Pavich, M., and four others: Using cosmogenic nuclides to contrast rates of erosion and sediment yield in a semi-arid, arroyo-dominated landscape, Rio Puerco Basin, New Mexico, *Earth Surf. Proc. Land.*, 30, 935-953, 2005.
- Box, G. E. P., and Draper, N.: *Empirical model building and response surfaces*, Wiley, 688, 1987.
- Briner, J. P., Kaufman, D. S., Manley, W. F., Finkel, R. C., and Caffee, M. W.: Cosmogenic exposure dating of late Pleistocene moraine stabilization in Alaska, *Geol. Soc. Am. Bull.*, 117, 1108-1120, 2005.
- Brown, E. T., Molnar, P., and Bourlés, D. L.: Comment on "Slip-rate measurements on the Karakorum Fault may imply secular variations in fault motion", *Science*, 309, 1326b, 2005.
- Chambers, J. M., Cleveland, W. S., Kleiner, B., and Tukey, J. W.: *Graphical methods for data analysis*: Wadsworth, 395, 1983.
- Chevalier, M.-L., Ryerson, F. J., Tapponier, P., and four others: Slip-rate measurements on the Karakorum Fault may imply secular variations in fault motion: *Science*, 307, 411-414, 2005.
- Croarkin, C., and Tobias, P. (eds.): *NIST/SEMATECH e-Handbook of Statistical Methods*, <http://www.itl.nist.gov/div898/handbook/>, accessed 18 September 2009, 2006.
- Dyurgerov, M. B., and Meier, M. F.: *Twentieth century climate change: evidence from small glaciers*, *P. Natl. Acad. Sci. USA*, 97, 1406-1411, 2000.

- Dreimanis, A.: Tills: their genetic terminology and classification, in: Genetic classification of glacial deposits, Balkema, 17-84, 1988.
- Dunne, J., Elmore, D., and Muzikar, P.: Scaling factors for the rates of production of cosmogenic nuclides for geometric shielding and attenuation at depth on sloped surfaces, *Geomorphology*, 27, 3-11, 1999.
- Fletcher, C. A. J.: Computational techniques for fluid dynamics, volume 1 (2nd ed.), Springer, 401, 1991.
- Gibbons, A. B., Megeath, J. D., and Pierce, K. L.: Probability of moraine survival in a succession of glacial advances, *Geology*, 12, 327-330, 1984.
- Gosse, J. C., Klein, J., Evenson, E. B., Lawn, B., and Middleton, R.: Beryllium-10 dating of the duration and retreat of the last Pinedale glacial sequence, *Science*, 268, 1329-1333, 1995a.
- Gosse, J. C., Evenson, E. B., Klein, J., Lawn, B., and Middleton, R.: Precise cosmogenic  $^{10}\text{Be}$  measurements in western North America: support for a global Younger Dryas cooling event, *Geology*, 23, 877-880, 1995b.
- Gosse, J. C., and Phillips, F. M.: Terrestrial in situ cosmogenic nuclides: theory and application, *Quaternary. Sci. Rev.*, 20, 1475-1560, 2001.
- Granger, D. E., and Muzikar, P. F.: Dating sediment burial with in situ-produced cosmogenic nuclides: theory, techniques, and limitations, *Earth Planet. Sci. Lett.*, 188, 269-281, 2001.
- Granger, D. E., Fabel, D., and Palmer, A. N.: Pliocene-Pleistocene incision of the Green River, Kentucky, determined from radioactive decay of cosmogenic  $^{26}\text{Al}$  and  $^{10}\text{Be}$  in Mammoth Cave sediments, *Geol. Soc. Amer. Bull.*, 113, 825-836, 2001.
- Hallet, B., and Putkonen, J.: Surface dating of dynamic landforms: young boulders on aging moraines, *Science*, 265, 937-940, 1994.
- Hanks, T.: The age of scarplike landforms from diffusion-equation analysis, in: Quaternary geochronology: methods and applications, American Geophysical Union Reference Shelf, 4, American Geophysical Union, 2000.
- Heisinger, B., Lal, D., Jull, A. J. T., and six others: Production of selected cosmogenic radionuclides by muons 1. Fast muons, *Earth Planet. Sci. Lett.*, 200, 345-355, 2002a.
- Heisinger, B., Lal, D., Jull, A. J. T., and four others: Production of selected cosmogenic radionuclides by muons 2. Capture of negative muons, *Earth Planet. Sci. Lett.*, 200, 357-369, 2002b.
- Hilborn, R., and Mangel, M.: The ecological detective: confronting models with data, Monographs in Population Biology, 28, Princeton University Press, 315, 1997.
- Ivy-Ochs, S., Kerschner, H., and Schlüchter, C.: Cosmogenic nuclides and the dating of Lateglacial and early Holocene glacier variations: the Alpine perspective, *Quatern. Int.*, 164-165, p. 53-63, 2007.

Jansen, E., Overpeck, J., Briffa, K. R., and 13 others: Paleoclimate, in: *Climate change 2007: the physical science basis: contribution of Working Group I to the Fourth Assessment Report of the Intergovernmental Panel on Climate Change*, Cambridge University Press, 433-498, 2007.

Kaplan, M. R., Douglass, D. C., Singer, B. S., Ackert, R. P., and Caffee, M. W.: Cosmogenic nuclide chronology of pre-last glacial maximum moraines at Lago Buenos Aires, 46°S, Argentina, *Quaternary Res.*, 63, 301-315, 2005.

Kelly, M. A., Lowell, T. V., Hall, B. L., and five others: A  $^{10}\text{Be}$  chronology of lateglacial and Holocene mountain glaciation in the Scoresby Sund region, east Greenland: implications for seasonality during lateglacial time, *Quaternary Sci. Rev.*, 27, 2273-2282, 2008.

Kowalski, S. E., Lowell, T. V., and Evenson, E. B., in preparation, Major ice collapse (17 ka – 16 ka) in the Anchorage lowland, southern Alaska, *Quaternary Res.*, in preparation.

Krüger, J.: Moraine ridges formed from subglacial frozen-on sediment slabs and their differentiation from push moraines, *Boreas*, 25, 57-63, 1996.

Lal, D.: Cosmic ray labeling of erosion surfaces: in situ nuclide production rates and erosion models, *Earth Planet. Sci. Lett.*, 104, 424-439, 1991.

Lal, D., and Chen, J.: Cosmic ray labeling of erosion surfaces II: special cases of exposure histories of boulders, soils, and beach terraces, *Earth Planet. Sci. Lett.*, 236, 797-813, 2005.

Licciardi, J. M., Clark, P. U., Brook, E. J., Elmore, D., and Sharma, P.: Variable responses of western U. S. glaciers during the last deglaciation, *Geology*, 32, 81-84, 2004.

Masarik, J., and Wieler, R.: Production rates of cosmogenic nuclides in boulders, *Earth Planet. Sci. Lett.*, 216, 201-208, 2003.

Murphy, E. A.: One cause? Many causes? The argument from the bimodal distribution, *J. of Chron. Dis.*, 17, 301-324, 1964.

Muzikar, P.: General models for episodic surface denudation and its measurement by cosmogenic nuclides, *Quaternary Geochronol.*, v. 4, p. 50-55, 2009.

Nash, D. B.: Morphologic dating and modeling degradation of fault scarps, in: *Active Tectonics*, National Academy Press, 266, 1986.

Oerlemans, J.: Extracting a climate signal from 169 glacier records: *Science*, v. 308, p. 675-677, 2005.

O'Neal, M. A.: The effects of slope degradation on lichenometric dating of Little Ice Age moraines, *Quaternary Geochronol.*, 1, 121-128, 2006.

Pelletier, J. D., DeLong, S. B., al-Suwaidi, A. H., and four others: Evolution of the Bonneville shoreline scarp in west-central Utah: comparison of scarp-analysis methods and implications for the diffusion model of hillslope evolution, *Geomorphology*, 74, 257-270, 2006.

Pelletier, J. D., *Quantitative modeling of earth surface processes*: Cambridge University Press, 304, 2008.

- Press, W. H., Teukolsky, S. A., Vetterling, W. T., and Flannery, B. P.: Numerical recipes in Fortran 77 (2nd ed.), Cambridge, 927, 1992.
- Putkonen, J., and Swanson, T.: Accuracy of cosmogenic ages for moraines, *Quaternary Res.*, 59, 255-261, 2003.
- Putkonen, J., Connolly, J., and Orloff, T.: Landscape evolution degrades the geologic signature of past glaciations, *Geomorphology*, v. 97, p. 208-217, 2007.
- Richmond, G. M.: Geologic map of the Fremont Lake South quadrangle, Sublette County, Wyoming, 1:50,000, U. S. Geological Survey Geologic Quadrangle Map GQ-1138, 1973.
- Roering, J. J., Kirchner, J. W., Sklar, L. S., and Dietrich, W. E.: Hillslope evolution by nonlinear creep and landsliding: an experimental study, *Geology*, 29, 143-146, 2001.
- Schaefer, J. M., Oberholzer, P., Zhao, Z., and five others: Cosmogenic beryllium-10 and neon-21 dating of late Pleistocene glaciations in Nyalam, monsoonal Himalayas, *Quaternary Sci. Rev.*, 27, 295-311, 2008.
- Seong, Y. B., Owen, L. A., Caffee, M. W., and five others: Rates of basin-wide rockwall retreat in the K2 region of the central Karakoram defined by terrestrial cosmogenic nuclide  $^{10}\text{Be}$ , *Geomorphology*, 107, 254-262, 2009.
- Shackleton, N. J.: The 100,000-year ice-age cycle identified and found to lag temperature, carbon dioxide, and orbital eccentricity, *Science*, 289, 1899-1902, 2000.
- Wolkowinsky, A. J., and Granger, D. E.: Early Pleistocene incision of the San Juan River, Utah, dated with  $^{26}\text{Al}$  and  $^{10}\text{Be}$ : *Geology*, v. 32, p. 749-752, 2004.
- Zimmerman, S. G., Evenson, E. B., Gosse, J. C., and Erskine, C. P.: Extensive boulder erosion resulting from a range fire on the type-Pinedale moraines, Fremont Lake, Wyoming, *Quaternary Research*, 42, 255-264, 1995.
- Zreda, M. G., Phillips, F. M., and Elmore, D.: Cosmogenic  $^{36}\text{Cl}$  accumulation in unstable landforms 2. Simulations and measurements on eroding moraines, *Water Resources Research*, 30, 3127-3136, 1994.

## Figures

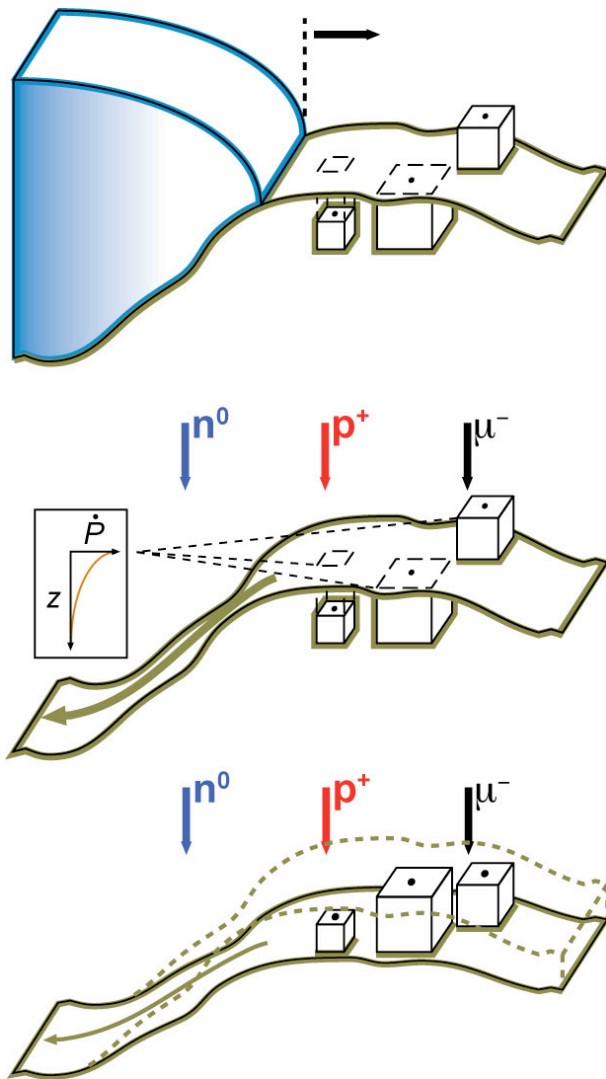


**Figure 1:** Conceptual model of moraine degradation.

Top: An advancing glacier margin constructs a new moraine. Some boulders, shown as cubes, are buried, whereas other boulders rest on the surface of the moraine.

Middle: The glacier margin retreats, abandoning the moraine. Several processes begin. The boulders begin to accumulate cosmogenic nuclides as they are bombarded by cosmic rays, shown as arrows. The cosmic ray flux is made up of neutrons ( $n^0$ ), protons ( $p^+$ ), and negative muons ( $\mu^-$ ). The production rate in each boulder depends on its burial depth; boulders at the surface accumulate nuclides most rapidly, and the production rate falls off exponentially with depth, as shown in the inset panel. At the same time that the boulders accumulate nuclides, loose sediment moves downhill.

Bottom: After some period of time, many boulders are on the moraine surface, including a large number that were originally buried. The moraine slope has diminished, and so has the downhill flux of sediment. The original surface of the moraine is shown as a dashed line. Eventually, the boulders are sampled, yielding a wide range of exposure dates.

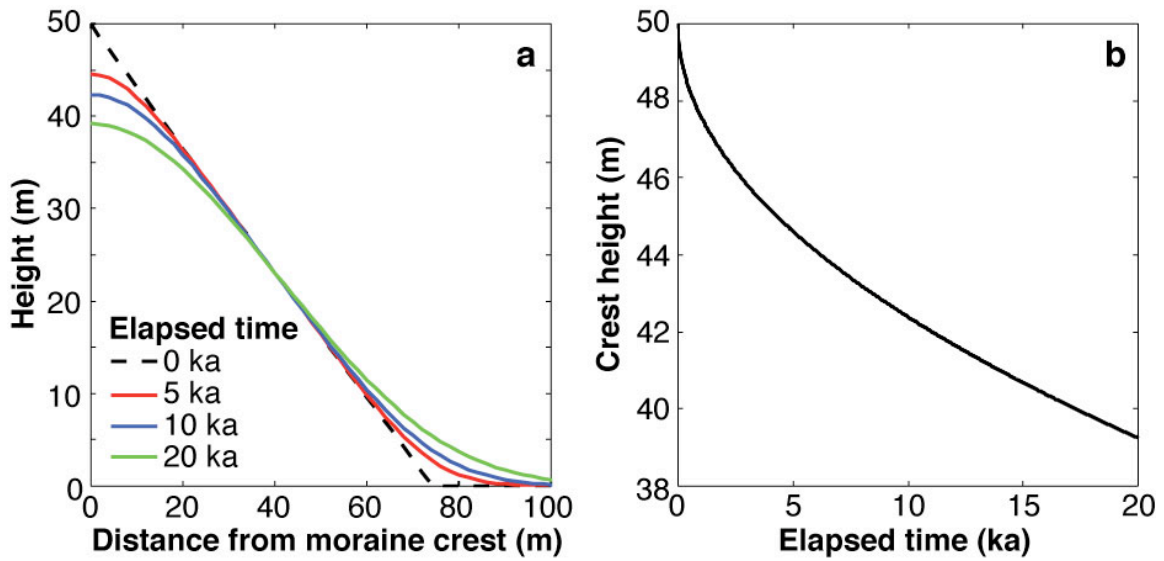


**Figure 2:** Evolution of moraine profile with time (a) and change in height of moraine with time (b) for a representative case. As time goes on, the moraine's profile changes most at the crest and at the toe of the slope, becoming generally more rounded. As material is transported from the crest to the toe of the slope, the moraine becomes shorter. The moraine loses height rapidly at first, then more slowly. In (a), only one-half of the moraine's profile is shown; the modeled moraine is symmetrical about the  $y$ -axis. Note that the moraine loses more than 10 m of its initial height over 20 ka. Compare (a) to Figure 1 of Hallet and Putkonen (1994); compare (b) to Figure 1 of Putkonen and Swanson (2003). In this figure, the moraine's initial height is 50 m, its initial slope is  $34^\circ$ , and its topographic diffusivity is  $10^{-2} \text{ m}^2/\text{yr}$ .

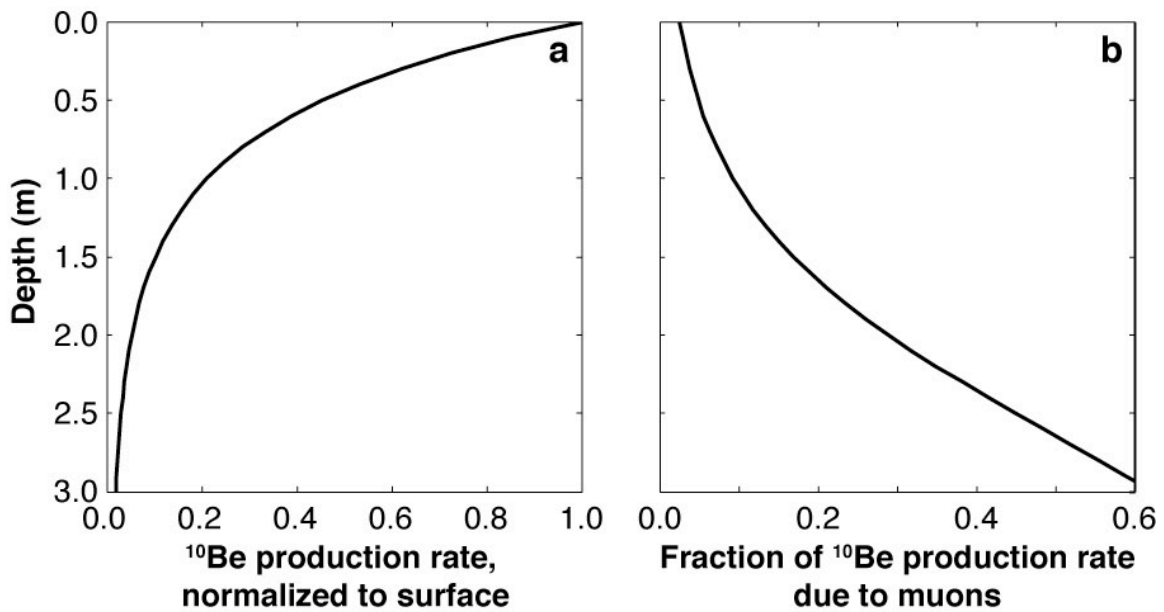


**Figure 3:** Production rate of beryllium-10 with depth (a) and fraction of beryllium-10 production due to muons as a function of depth (b) in quartzite, following Granger and Muzikar (2001). The total production rate of beryllium-10 is roughly exponential as a function of depth; production is greatest at the surface, and falls off below the surface with an  $e$ -folding length of a few tens of centimeters (Lal, 1991). Most production near the surface is caused by high-energy protons and neutrons, which produce beryllium-10 by splitting atoms of oxygen and silicon in quartz (Gosse and Phillips, 2001). At greater depths, most production is due to muons, which do not interact with target atoms in the rock as easily as high-energy protons and neutrons. Compare this figure to Figure 2a of Gosse and Phillips (2001). This figure assumes surface beryllium-10 production rates corresponding to sea level and high latitude and a rock density of  $2.65 \text{ g/cm}^3$ .

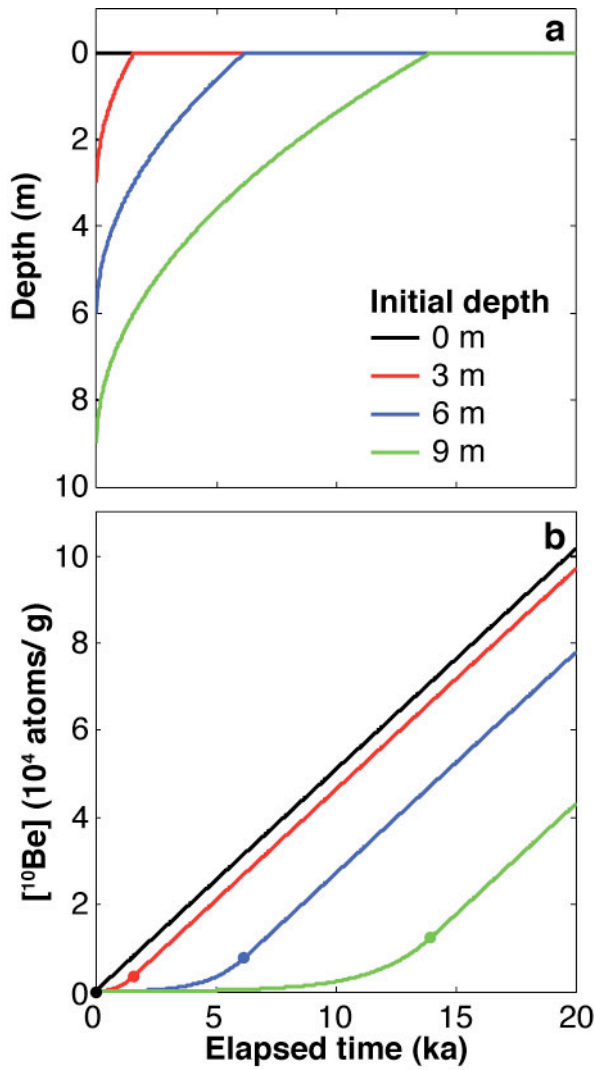


**Figure 4:** Depths of boulders in a degrading moraine over time (a) and beryllium-10 concentrations in the same boulders as a function of time (b). If boulders are uniformly distributed throughout the till, then some boulders will be at the surface when the moraine is deposited, whereas other boulders will be present in the till at greater depths. As time goes forward, the moraine becomes shorter (Fig. 2), and the boulders approach the surface. At the same time, cosmogenic nuclides are produced in the boulders (Fig. 3). For buried boulders, production rates increase slowly as the surface lowers, then become constant after the boulders are exposed at the surface. Note that the majority of the cosmogenic nuclides in each boulder are produced after the boulder reaches the surface, even for the most deeply buried boulder. In (b), the dots indicate the time when each boulder reaches the surface. As in Figure 2, the moraine's initial height is 50 m, its initial slope is  $34^\circ$ , and its topographic diffusivity is  $10^{-2} \text{ m}^2/\text{yr}$ . The final heights of all the boulders are 1 m.

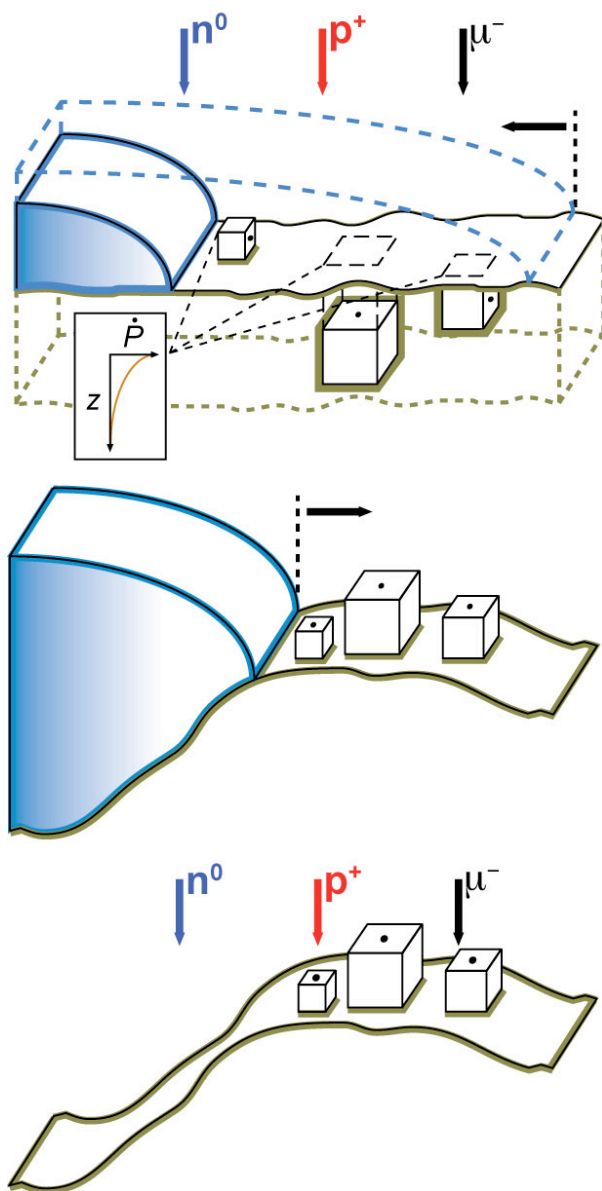


**Figure 5:** Conceptual model of inheritance, as caused by boulder reworking.

Top: A retreating glacier margin deposits a till carpet on its former bed. The till carpet is outlined in dashed, brown lines. Some boulders, shown as cubes, are distributed throughout the till carpet. The boulders contain different concentrations of cosmogenic nuclides, depending on their depth in the till carpet and the length of time since the margin of the ice sheet uncovered the overlying till surface. The dot on each boulder represents the point that will eventually be sampled for cosmogenic nuclides.

Middle: The glacier readvances, eroding to some depth within the till carpet and incorporating the boulders into a new moraine. Glacial transport rotates the boulders to their final orientations.

Bottom: The glacier margin abandons the new moraine, and the boulders accumulate more cosmogenic nuclides. Eventually, the boulders are sampled, yielding a wide range of exposure dates.

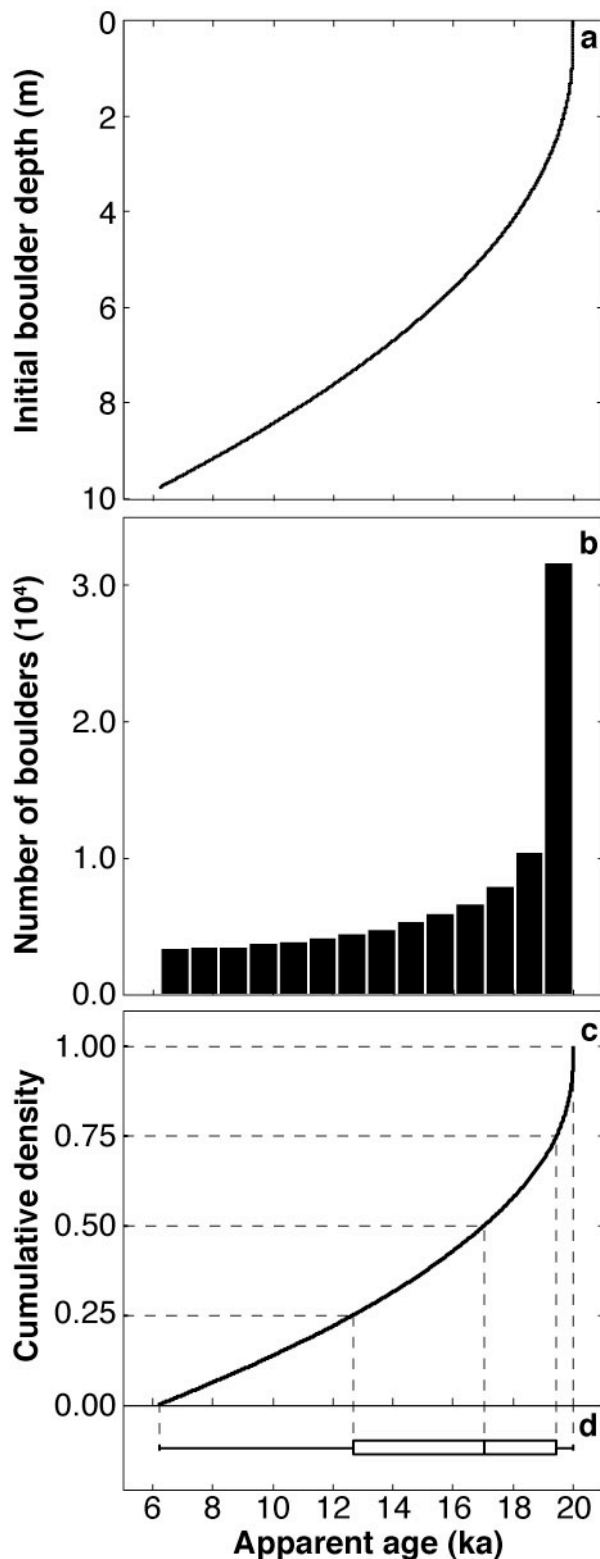


**Figure 6:** Distribution of cosmogenic exposure dates produced by the moraine degradation model for a representative case. Panel (a) shows the exposure dates yielded by boulders as a function of their initial burial depth in the moraine (compare Fig. 4b). Panel (b) shows a histogram of these apparent ages. Most of the exposure dates cluster around the true age of the moraine (20 ka), but there is a long, heavy tail to the left. That is, the distribution of exposure dates produced by the moraine degradation model is left-skewed. The total number of observations shown in this histogram is  $10^5$ . Panels (c) and (d) show the cumulative density function and box plot of the  $10^5$  observations shown in the histogram. Dashed lines in (c) and (d) show the relationship of the box plot to the cumulative density function; breaks in the box plot represent the quartiles of the distribution (Chambers et al., 1983). As in Figures 2 and 4, the moraine's initial height is 50 m, its initial slope is  $34^\circ$ , and its topographic diffusivity is  $10^{-2} \text{ m}^2/\text{yr}$ . The final heights of all the boulders are 1 m.

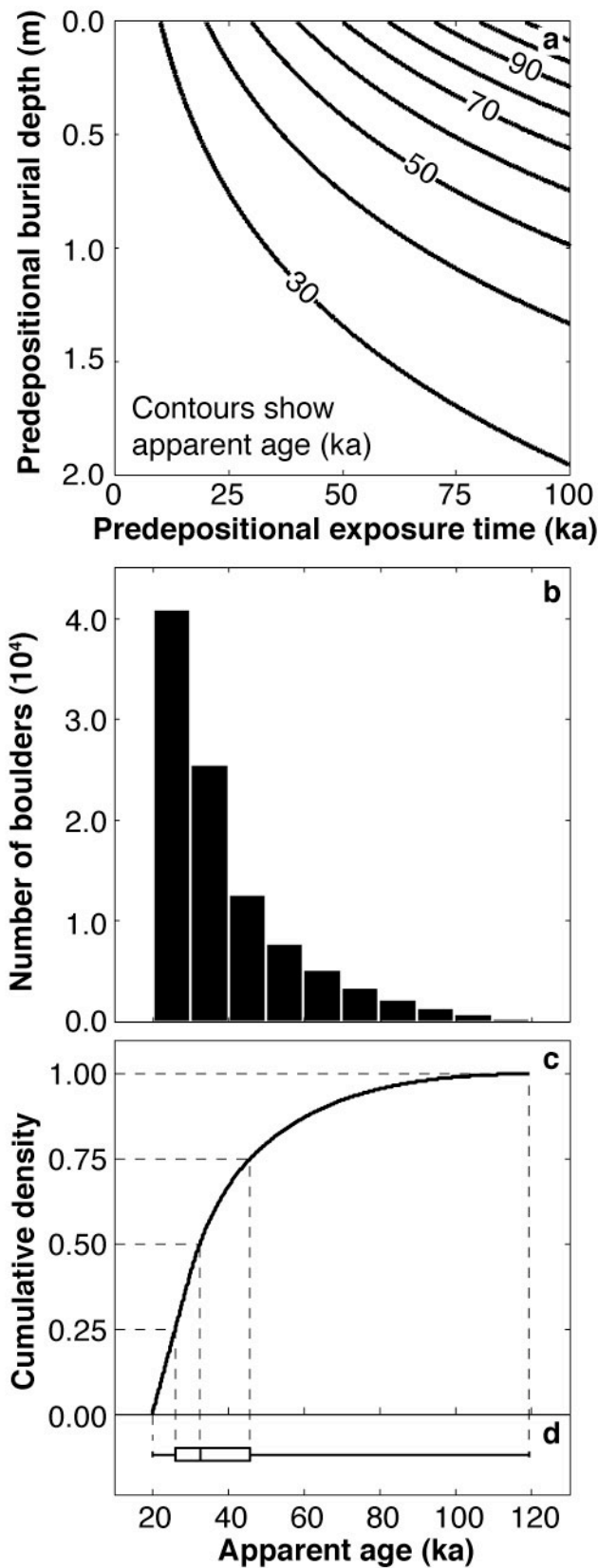


**Figure 7:** Distribution of cosmogenic exposure dates produced by the inheritance model for a representative case. Panel (a) shows contours of the apparent ages yielded by boulders as a function of the length of time that they were exposed to cosmic rays and the depth to which they were buried during that time. Panel (b) shows a histogram of exposure dates produced by random sampling of  $10^5$  synthetic observations from the contour plot in (a). In contrast to the distribution produced by the moraine degradation model (Fig. 6), the inheritance model produces right-skewed distributions. The bulk of the exposure dates fall near the true age of the moraine (20 ka), but there is a long, heavy tail to the right. Panels (c) and (d) show the cumulative density function and box plot of the  $10^5$  observations shown in the histogram. The true age of the moraine is 20 ka, the maximum predepositional exposure time is 100 ka, and the maximum predepositional burial depth is 2.0 m.

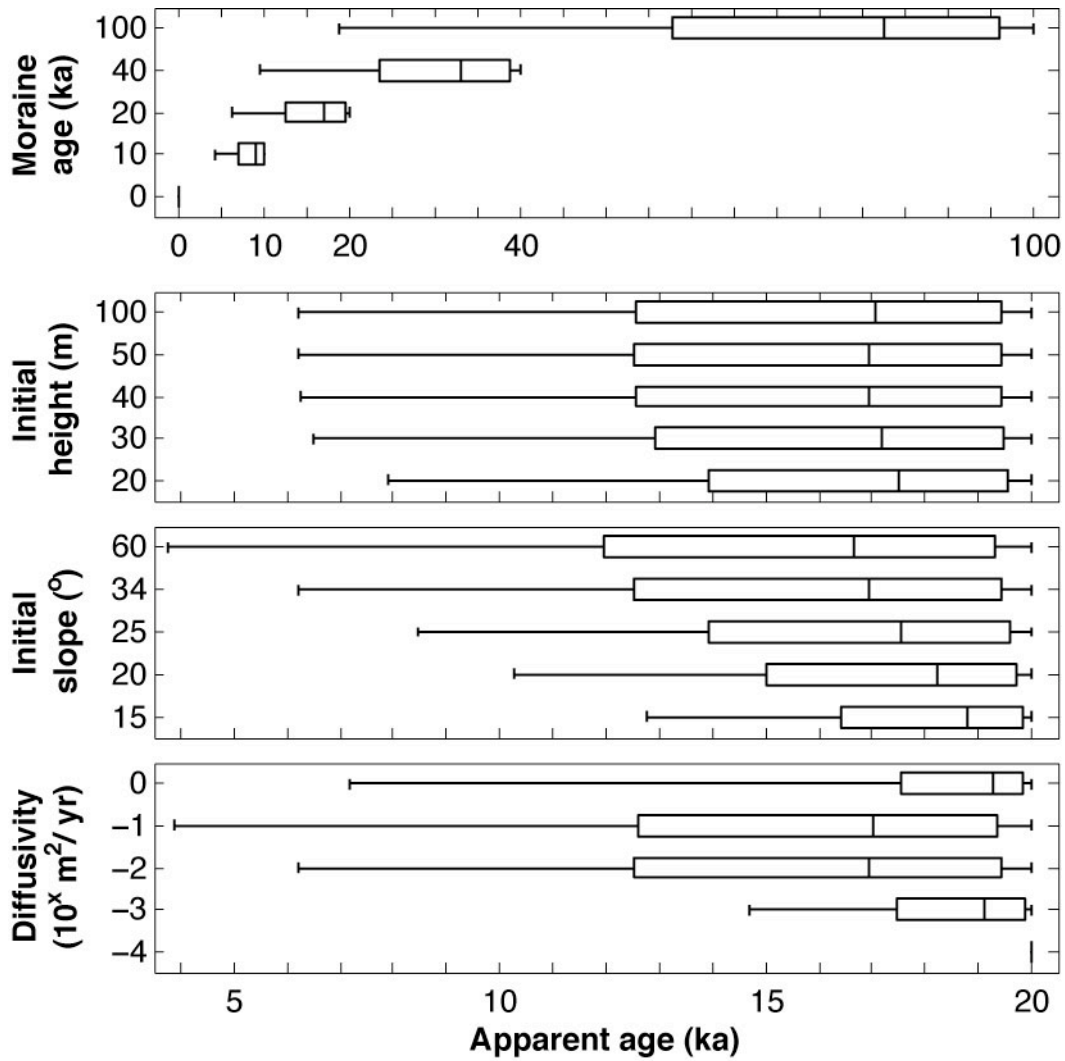


**Figure 8:** Sensitivity of the moraine degradation model to changes in its input parameters. See text for discussion. In each panel, one of the model parameters is varied between the values shown on the y-axis, whereas the other model parameters are held constant at the base values. As in Figures 2, 4, and 6, the base values for the input parameters specify that the moraine’s initial height is 50 m, its initial slope is 34°, and its topographic diffusivity is  $10^{-2} \text{ m}^2/\text{yr}$ .

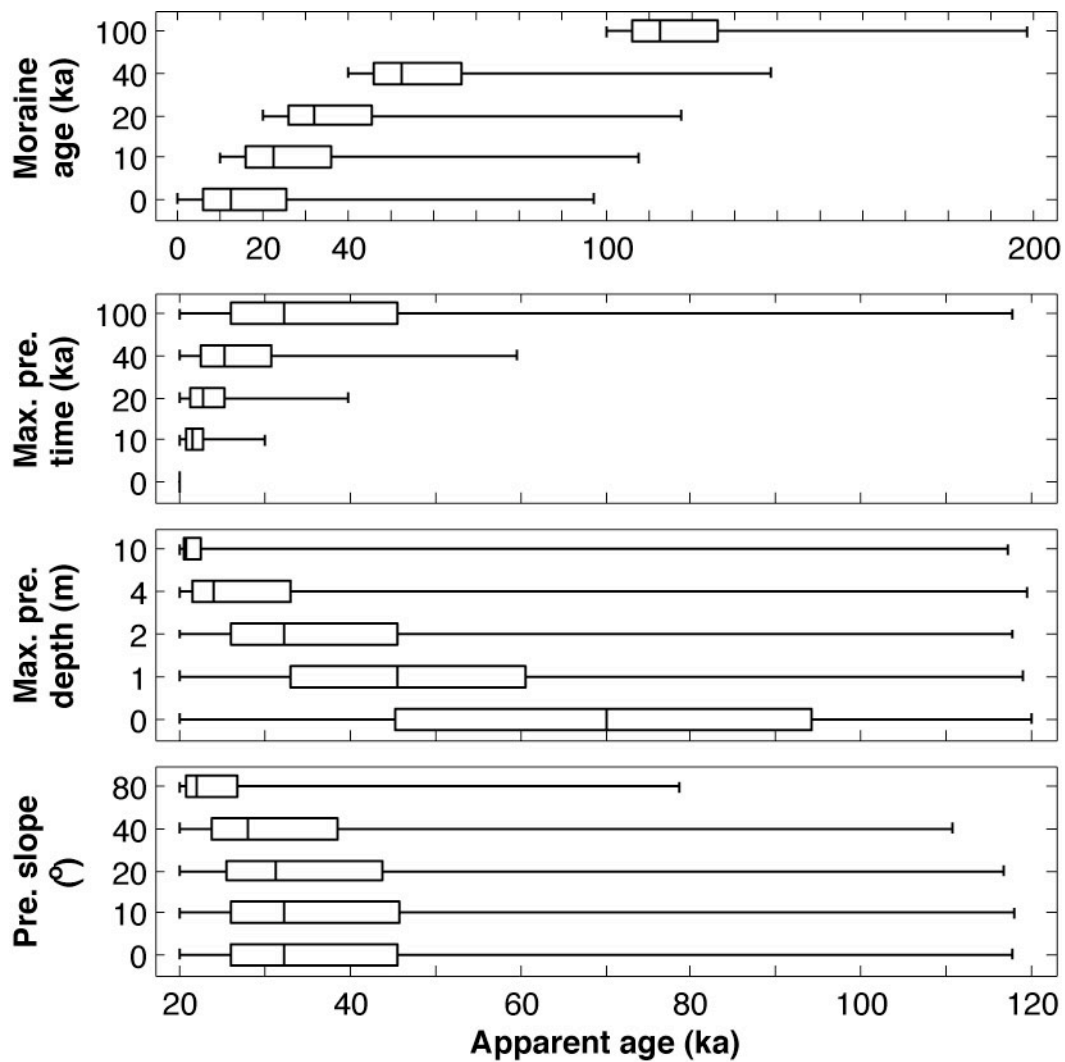


**Figure 9:** Sensitivity of the inheritance model to changes in its input parameters. See text for discussion. In each panel, one of the model parameters is varied between the values shown on the y-axis, whereas the other model parameters are held constant at the base values. As in Figure 7, the base values for the input parameters specify that the true age of the moraine is 20 ka, the maximum predepositional exposure time is 100 ka, and the maximum predepositional burial depth is 2.0 m.

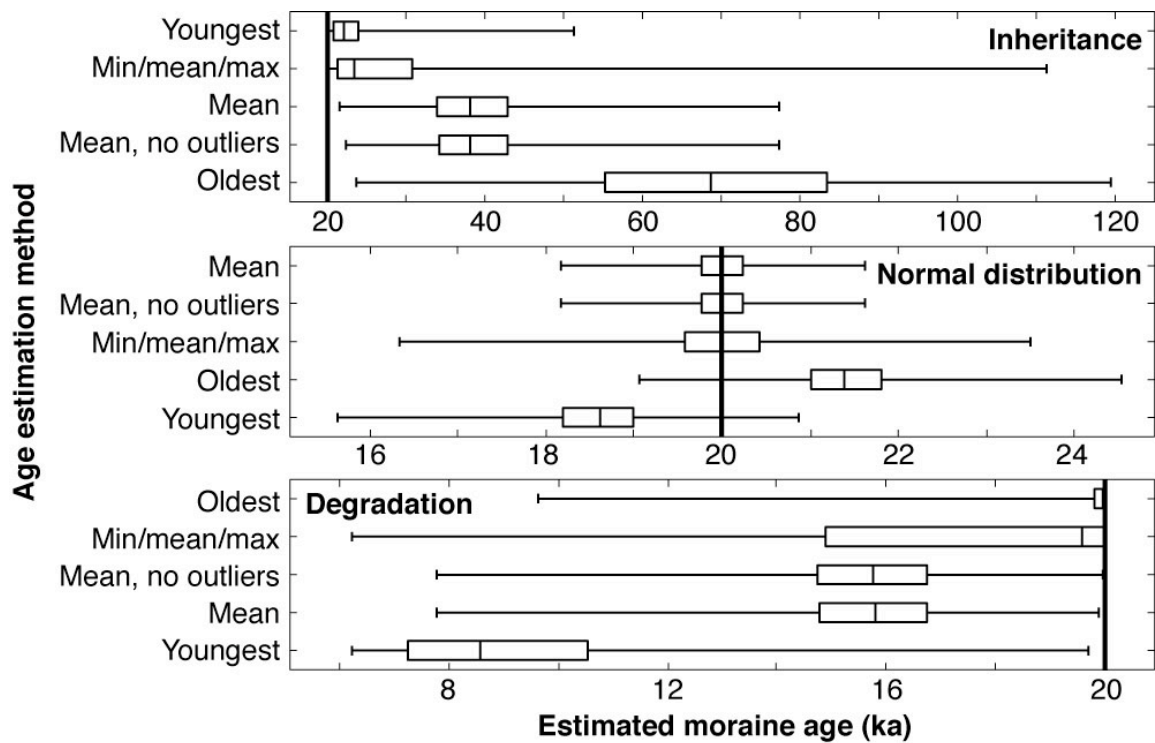


**Figure 10:** The reliability of different interpretive methods in estimating moraine ages from collections of cosmogenic exposure dates. Each box plot represents age estimates from  $10^6$  randomly selected data sets containing eight synthetic cosmogenic exposure dates each. The heavy, vertical black line in each panel represents the true age of the moraine, which is 20 ka in each case. In each panel, the methods listed on the y-axis are listed according to how close the median age estimate falls to the true moraine age; the method listed at the top is the best for the indicated parent distribution, and the method listed at the bottom is the worst. This ordering is insensitive to the number of samples in each data set for reasonable data set sizes ( $3 \leq n \leq 21$ ). The parent distribution in the middle panel is a normal distribution with a mean of 20 ka and a standard deviation of 1 ka, corresponding to a case where all of the scatter between the exposure dates is due to measurement error. The parent distributions in the other two panels are those shown in Figures 6 and 7.

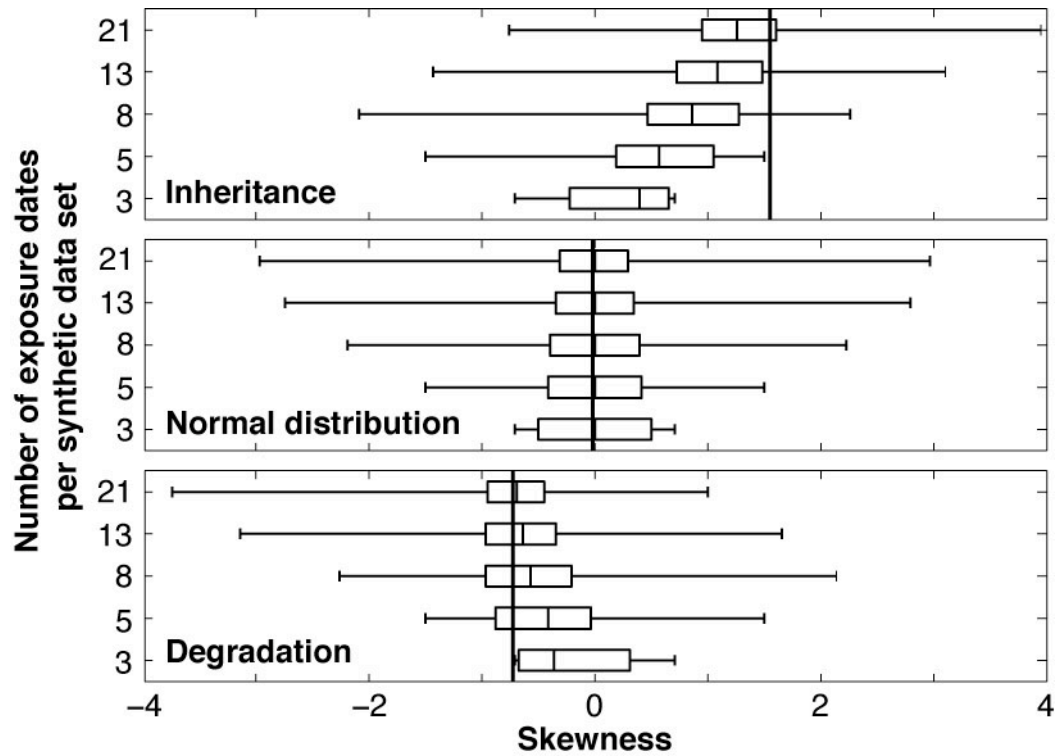


**Figure 11:** Skewnesses of randomly chosen data sets, compared to the skewnesses of the underlying parent distributions. Each box plot indicates the skewnesses of  $10^6$  randomly selected data sets that contain a number of exposure dates indicated by the corresponding value on the  $y$ -axis. The skewnesses of the underlying parent distributions are indicated by the heavy, black, vertical line in each panel. Even large data sets ( $n = 21$ ) can provide a misleading estimate of the skewness of the parent distribution. In particular, randomly chosen data sets will often yield skewnesses that do not have the same sign as the underlying parent distribution. The parent distribution in the top panel is the same as that shown in Figure 7b; the parent distribution in the bottom panel is shown in Figure 6b. The parent distribution in the middle panel is a normal distribution with a mean of 20 ka and a standard deviation of 1 ka.

## Model documentation for “Modeling the statistical distributions of cosmogenic exposure dates from moraines”

Applegate, P. J., Urban, N. M., Keller, K. K., and Alley, R. B.  
Correspondence to: P. J. Applegate (pappleaga@geosc.psu.edu)

### Overview

The codes given here are numerical models that describe the influence of moraine degradation and inheritance on the statistical distributions of cosmogenic exposure dates from glacial landforms, especially moraines. These two processes are treated in separate models, so the degradation model and the inheritance model reside in distinct files.

These codes were written in MATLAB version R2008a, and were run on an Intel-based Macintosh MacBook.

These codes were written carefully, and they have been checked for obvious errors. However, no warranty of any kind is implied. These codes may not even run on your system. The output from these codes should not be trusted without testing.

Please give proper credit if using these codes in research or teaching. Derivative works based on this code should include a reference to the original paper.

### Included files

#### *Model codes*

All these files are in the MATLAB .m file format. They can be read by any text editor. The freeware editor gedit will highlight the code in the same way as MATLAB’s integrated editor.

<u>File name</u>	<u>Description</u>
degradation_model.m	Main file for degradation model; calls the function m_diffusion.m
m_diffusion.m	Contains the part of the code that describes how moraine profiles change over time; based on a derivation prepared by Dr. Nathan Urban, Penn State
inheritance_model.m	Main file for inheritance model

#### *Representative output*

These files are in .csv (Comma Separated Values) format. Many of these files are too large to open in Microsoft Excel. Note that the values in these files have been rounded to 5 significant figures.

In the file names, the independent variable or variables are shown in parentheses, and the dependent variables are outside the parentheses. In the files themselves, the first column contains the independent variable, and the second column contains the dependent variable. Where there is more than one independent variable, the first few columns contain their values; the order corresponds to the order of the variable names in parentheses in the file names.

Thus, in the file `naive_age(initial_depth).csv`, the first column contains the initial depth values, and the second column contains the naive age values. In the file `naive_age(pre_time, pre_depth).csv`, the first column is `pre_time`, the second column is `pre_depth`, and the third is `naive_age`.

<u>File name</u>	<u>Description</u>
<b>Degradation model</b>	
<code>naive_age(initial_depth).csv</code>	Cosmogenic exposure dates generated by the degradation model for representative parameter values (see below). These exposure dates are represented as a function of the boulders' initial depths within the moraine.
<code>initial_profile(distances).csv</code> <code>final_profile(distances)_5ka.csv</code> <code>final_profile(distances)_10ka.csv</code> <code>final_profile(distances)_20ka.csv</code>	Elevation of a degrading moraine's surface above its base as a function of distance from the moraine's crest, at elapsed times of 0 ka, 5 ka, 10 ka, and 20 ka.
<code>crest_height(times).csv</code>	Height of a degrading moraine's crest above its base as a function of elapsed time, up to 20 ka.
<b>Inheritance model</b>	
<code>naive_age(pre_time, pre_depth).csv</code>	Cosmogenic exposure dates generated by the inheritance model for representative parameter values (see below). These exposure dates are represented as a function of the boulders' predepositional exposure times and their burial depths within the landscape during that time.

## The moraine degradation model (degradation\_model.m)

### *Input parameters*

The user-adjustable input parameters are contained in the same file as the model code, `degradation_model.m`. The values of these parameters are defined in lines 31-87.

<u>Name</u>	<u>Line</u>	<u>Default value</u>	<u>Symbol in text of paper</u>	<u>Description</u>
moraine_age	32	20 ka		Age of moraine (ka)
initial_height	33	50 m	$h_0$	Initial height of moraine (m)
initial_slope	34	34°	$\tan^{-1}(S_0)$	Initial slope of moraine flanks; note that the variable <code>initial_slope</code> is the slope angle, whereas $S_0$ in the text of the paper is the slope (rise over run). Few measurements of this parameter exist in the literature; see Hallet and Putkonen (1994), Putkonen and Swanson (2003), and Putkonen and O'Neal (2006).
k	39	$10^{-2}$ m <sup>2</sup> /yr (range: $10^{-4}$ to $10^{-1}$ )	$k$	Topographic diffusivity (m <sup>2</sup> /yr). See Hallet and Putkonen (1994), Hanks (2000), Putkonen and Swanson (2003), and Putkonen et al. (2007).
erosion_rate	42	0 mm/ka		Erosion rate of boulders when exposed at the moraine's surface (mm/ka)
boulder_height	43	1 m	$h_b$	Minimum sampled boulder height (m). The minimum boulder height that a field geomorphologist would sample.
rho_rock	44	2.6 g/cm <sup>3</sup>		Density of the boulders (g/cm <sup>3</sup> ); controls the $e$ -folding length of cosmic rays into the boulders.
rho_till	45	2.0 g/cm <sup>3</sup>		Density of the unconsolidated sediment surrounding the boulders; controls the $e$ -folding length of cosmic rays into the till.
P_spall	48	4.97 atoms <sup>10</sup> Be/g/yr	$P_{i=1}$	Production rate of cosmogenic nuclide by spallation at the earth's surface at the latitude and elevation of the study site. Get this from Balco et al. (2008), using the St scaling model.
P_mu	53	0.133 atoms <sup>10</sup> Be/g/yr	$\Sigma(P_{i=2,3,4})$	Production rate of cosmogenic nuclide by muons at the earth's surface at the latitude and elevation of the study site. Get this from Balco et al. (2008).
decay_const	56	$4.67 \cdot 10^{-7}$	$\lambda$	Decay constant of the cosmogenic

		$\text{yr}^{-1}$ (?) for $^{10}\text{Be}$		nuclide. For $^{10}\text{Be}$ , this value is in dispute (Balco et al., 2008, and refs therein), but this parameter has little effect on $^{10}\text{Be}$ exposure dating over the time scales of interest ( $10^2$ - $10^5$ yr).
P_slhl	59	[5, 0.09, 0.02, 0.02] atoms $^{10}\text{Be}/\text{g}/\text{yr}$	$P_{i=1, 2, 3, 4}$	Surface production rates of nuclide at sea level and high latitude for various production pathways; see Granger and Muzikar (2001).
att_length	64	[160, 738, 2688, 4360] $\text{g}/\text{cm}^2$	material density* $\Lambda_{i=1, 2, 3, 4}$	Attenuation lengths of components of the cosmic ray flux; see Granger and Muzikar (2001). In the text, $\Lambda_{i=1, 2, 3, 4}$ are these values, divided by the density (in $\text{g}/\text{cm}^3$ ) of the material the cosmic rays are passing through.
num_boulders	71	$10^5$ boulders		Number of boulders to simulate; more boulders produce a more robust distribution of exposure dates, but also cause the model to run more slowly.
time_step	75	25-100 yr		Controls fineness of model discretization in time; smaller values produce more accurate results, but also cause the model to run more slowly.
plots	82	0 or 1		If 0, the code produces no plots; if 1, the plots described below are generated.
bin_width	87	1-5 ka		If plots = 1, this variable controls the widths of the bins into which the calculated exposure dates are sorted to create the histogram (see below).

### Output

The degradation model places its output into the following variables.

<u>Name</u>	<u>Line</u>	<u>Symbol in text of paper</u>	<u>Description</u>
initial_profile	109	$z(x, t = 0)$	Initial height of the moraine above its base as a function of distance from the crest (m).
final_profile	109	$z(x, t)$	Final height of the moraine above its base as a function of distance from the crest (m).
crest_height	109	$z(x = 0, t)$	Height of the moraine's crest above its base as a function of time.
distances	109	$x$	A plotting variable that contains evenly spaced values of distance from the moraine crest (m).
times	109	$t$	A plotting variable that contains evenly spaced values of time from the beginning of the simulation (yr or ka).
initial_depth	116	$d_0$	Initial burial depth of each boulder in the moraine

			(m).
naive_age	171	$t_{app}$	Apparent exposure time yielded by each boulder (yr or ka).

If the variable plots is set to 1, the degradation model also produces plots of these variables. The plots show the initial and final profile of the moraine (initial\_profile and final\_profile vs. distances), the height of the moraine crest as a function of time (crest\_height vs. times), and a histogram of the exposure dates simulated by the model (naive\_age).

Numerical output from the degradation model is stored in the .csv files listed near the beginning of this document. These files generally assume a moraine age of 20 ka, an initial moraine height of 50 m, an initial slope of 34°, and a topographic diffusivity of  $10^{-2}$  m<sup>2</sup>/yr. The moraine profile for intermediate times (5 and 10 ka) is also given, assuming the other parameters have the same values.

## The inheritance model

(inheritance\_model.m)

### Input parameters

Many of the inheritance model's parameters are the same as those used in the degradation model.

<u>Name</u>	<u>Line</u>	<u>Default value</u>	<u>Symbol in text of paper</u>	<u>Description</u>
moraine_age	27	20 ka		Age of moraine (ka)
max_pre_time	28	100 ka	$\max(t_{\text{pre}})$	Maximum predepositional exposure time for the boulders (ka).
max_pre_depth	30	2.0 m	$\max(d_{\text{pre}})$	Maximum predepositional burial depth for the boulders (m).
pre_slope	32	0°		Slope of surface from which preexposed boulders were derived (°).
erosion_rate		0 mm/ka		Erosion rate of boulders after being deposited on the moraine (mm/ka)
rho_rock	36	2.6 g/cm <sup>3</sup>		Density of the boulders (g/cm <sup>3</sup> ); controls the <i>e</i> -folding length of cosmic rays into the boulders.
rho_over	37	2.6 g/cm <sup>3</sup>		Density of material overlying the boulders during the predepositional exposure period (g/cm <sup>3</sup> ); controls the <i>e</i> -folding length of cosmic rays into the boulders during that time.
P_spall	42	4.97 atoms <sup>10</sup> Be/g/yr	$P_{i=1}$	Production rate of cosmogenic nuclide by spallation at the earth's surface at the latitude and elevation of the study site. Get this from Balco et al. (2008), using the St scaling model.
P_mu	47	0.133 atoms <sup>10</sup> Be/g/yr	$\Sigma(P_{i=2,3,4})$	Production rate of cosmogenic nuclide by muons at the earth's surface at the latitude and elevation of the study site. Get this from Balco et al. (2008).
decay_const	50	4.67* 10 <sup>-7</sup> yr <sup>-1</sup> (?) for <sup>10</sup> Be	$\lambda$	Decay constant of the cosmogenic nuclide. For <sup>10</sup> Be, this value is in dispute (Balco et al., 2008, and refs therein), but this parameter has little effect on <sup>10</sup> Be exposure dating over the time scales of interest (10 <sup>2</sup> -10 <sup>5</sup> yr).
P_slhl	53	[5, 0.09, 0.02, 0.02] atoms <sup>10</sup> Be/g/yr	$P_{i=1,2,3,4}$	Surface production rates of nuclide at sea level and high latitude for various production pathways; see Granger and Muzikar (2001).
att_length	58	[160, 738, 2688,	material density* $\Lambda_{i=1,2,3,4}$	Attenuation lengths of components of the cosmic ray flux; see Granger and Muzikar (2001). In the text, $\Lambda_{i=1,2,3,4}$ are

		4360]		these values, divided by the density (in g/cm <sup>3</sup> ) of the material the cosmic rays are passing through.
num_boulders	65	10 <sup>5</sup> boulders		Number of boulders to simulate; more boulders produce a more robust distribution of exposure dates, but also cause the model to run more slowly.
plots	71	0 or 1		If 0, the code produces no plots; if 1, the plots described below are generated.
bin_width	76	2-10 ka		If plots = 1, this variable controls the widths of the bins into which the calculated exposure dates are sorted to create the histogram (see below).

### *Output*

The inheritance model places its output into the following variables.

<u>Name</u>	<u>Line</u>	<u>Symbol in text of paper</u>	<u>Description</u>
pre_time	99	$t_{pre}$	Predepositional exposure time of each boulder (yr).
pre_depth	100	$d_{pre}$	Predepositional burial depth of each boulder (m).
naive_age	118	$t_{app}$	Apparent exposure time yielded by each boulder (yr or ka).

If the variable plots is set to 1, the model produces a histogram of the apparent exposure times.

Numerical output from the inheritance model is stored in the .csv file listed near the beginning of this document. This file assumes a moraine age of 20 ka, a maximum predepositional exposure time of 100 ka, and a predepositional burial depth of 2.0 m.